# Glutamate Substitution in Repeat IV Alters Divalent and Monovalent Cation Permeation in the Heart $Ca^{2+}$ Channel

L. Parent and M. Gopalakrishnan
Department of Molecular Physiology and Biophysics, Baylor College of Medicine, Houston, TX 77030 USA

ABSTRACT In voltage-gated ion channels, residues responsible for ion selectivity were identified in the pore-lining SS1-SS2 segments. Negatively charged glutamate residues (E393, E736, E1145, and E1446) found in each of the four repeats of the $\alpha_{1C}$ subunit were identified as the major determinant of selectivity in $Ca^{2+}$ channels. Neutralization of glutamate residues by glutamine in repeat I (E393Q), repeat III (E1145Q), and repeat IV (E1446Q) decreased the channel affinity for calcium ions 10-fold from the wild-type channel. In contrast, neutralization of glutamate residues in repeat II failed to significantly alter $Ca^{2+}$ affinity. Likewise, mutation of neighboring residues in E1149K and D1450N did not affect the channel affinity, further supporting the unique role of glutamate residues E1145 in repeat III and E1446 in repeat IV in determining $Ca^{2+}$ selectivity. Conservative mutations E1145D and E1446D preserved high-affinity $Ca^{2+}$ binding, which suggests that the interaction between $Ca^{2+}$ and the pore ligand sites is predominantly electrostatic and involves charge neutralization. Mutational analysis of E1446 showed additionally that polar residues could achieve higher $Ca^{2+}$ affinity than small hydrophobic residues could. The role of high-affinity calcium binding sites in channel permeation was investigated at the single-channel level. Neutralization of glutamate residue in repeats I, II, and III did not affect single-channel properties measured with 115 mM $BaCl_2$. However, mutation of the high-affinity binding site E1446 was found to significantly affect the single-channel conductance for $Ba^{2+}$ and $Li^+$, providing strong evidence that E1446 is located in the narrow region of the channel outer mouth. Side-chain substitutions at 1446 in repeat IV were used to probe the nature of divalent cation-ligand interaction and monovalent cation-ligand interaction in the calcium channel pore. Monovalent permeation was found to be inversely proportional to the volume of the side chain at position 1446, with small neutral residues such as alanine and glycine producing higher $Li^+$ currents than the wild-type channel. This suggests that steric hindrance is a major determinant for monovalent cation conductance. Divalent permeation was more complex. $Ba^{2+}$ single-channel conductance decreased when small neutral residues such as glycine were replaced by bulkier ones such as glutamine. However, negatively charged amino acids produced single-channel conductance higher than predicted from the size of their side chain. Hence, negatively charged residues at position 1446 in repeat IV are required for divalent cation permeation.

## INTRODUCTION

L-type $Ca^{2+}$ channels are highly selective for $Ca^{2+}$, but in completely multivalent-free conditions $Ca^{2+}$ channels will pass alkali metal ions at a remarkably high rate. However, monovalent cation inward permeation is blocked by the presence of external $Ca^{2+}$ at concentrations as low as 1 $\mu$M (Hess and Tsien, 1984; Almers et al., 1984; Lux et al., 1990). This experimental finding has long been explained by the existence of high-affinity $Ca^{2+}$ binding site(s) closely related to the channel selectivity mechanism. On the other hand, single-channel currents carried by increasing $Ca^{2+}$ concentration are known to saturate with an apparent dissociation constant of ~14 mM (Hess et al., 1986), which argues that permeation may be controlled by a different set of $Ca^{2+}$ binding sites. Altogether these results could imply that selectivity and permeation in $Ca^{2+}$ channels require at least two different sets of $Ca^{2+}$ binding sites, with their apparent affinity differing by four orders of magnitude.

During the last 10 yr, numerous models have been proposed to explain selectivity and permeation in native calcium channels (Almers and McCleskey, 1984; Hess et al., 1986; Armstrong and Neyton, 1992; Kuo and Hess, 1993a,b). The classic "two-site" model postulated two high-affinity $Ca^{2+}$ binding wells (≈1 $\mu$M) located in the middle of the permeation pathway (Tsien et al., 1987). As the external $Ca^{2+}$ concentration increases from the micromolar to the millimolar range, strong electric repulsions between cations are then responsible for promoting high fluxes (Tsien et al., 1987). In contrast, the "one-site" model proposed a single negatively charged (−2e) high-affinity binding site that would never be vacant under physiological conditions (Armstrong and Neyton, 1992). Permeation would be explained through knock-on or ion exchange between cations. During conduction, the ligand site would alternate between single and double occupancy, and the rate-limiting step would be the departure of a cation from the doubly occupied site. Both models, however, fail to explain the slow increase of conductance with divalent cation concentration reported by Yue and Marban (1990), which can only be explained by three or more $Ca^{2+}$ binding sites in the pore that can be occupied simultaneously. More recent experiments performed with destroyed cell-attached

*Received for publication 24 March 1995 and in final form 16 August 1995.*

Address reprint requests to Dr. Lucie Parent, Department of Molecular Physiology and Biophysics, Baylor College of Medicine, One Baylor Plaza, Houston, TX 77030. Tel.: 713-798-3889; Fax: 713-798-3475; E-mail: parent@phy.bcm.tmc.edu.

Dr. Gopalakrishnan's present address is Abbott Laboratories, Pharmaceutical Products Division, Abbott Park, Il 60064-3500.



0006-3495/95/11/1801/00 $2.00

patches with defined internal and external conditions provided additional support to multi-ion single-file permeation, with a few distinctions (Kuo and Hess, 1993a,b). Kuo and Hess (1993a,b) concluded that the pore must be asymmetrical, in contrast to the classic two-site model (Tsien et al., 1987; Rosenberg and Chen, 1991). In the Kuo-Hess model, the pore contains one set of high-affinity $Ca^{2+}$ binding sites facing the external medium that could be composed of at least two sites separated by insignificant barriers. Moreover, their findings argue strongly for a very short electrical distance between the external mouth of the channel and the high-affinity binding sites; other ionic sites should not be located external to the high-affinity sites (Kuo and Hess, 1993b). A minimum of two low-affinity nonspecific sites that loosely bind both $Ca^{2+}$ and $Li^{+}$ should also be located in the pore and closer to the inner face of the membrane than the high-affinity sites. Finally, the pore could contain at least three ions simultaneously distributed among high- and low-affinity sites, and ion-ion interactions would be responsible for ion movement through the pore.

Voltage-dependent ion channels, which include $Ca^{2+}$, $Na^{+}$, and $K^{+}$ channels, are members of a large multigene family of proteins that form ion conduction pathways across cell membranes. A combined approach using molecular biology and electrophysiology techniques has provided insights into the basic properties of the structure and function of these channels. Pioneer work performed on recombinant $K^{+}$ channels has identified the highly conserved linker region H5 between the transmembrane segments S5 and S6 as a major determinant of selectivity and conductance in voltage-dependent ion channels (Hartmann et al., 1991; Yool and Schwarz, 1991).

More recently, amino acids responsible for ion binding were identified in voltage-dependent $Ca^{2+}$ channels (Yang et al., 1993; Tang et al., 1993; Kim et al., 1993; Yatani et al., 1994) and in cyclic nucleotide-gated channels (Root and MacKinnon, 1993; Eismann, 1994). Both channels contain high-affinity, divalent cation binding sites that are important for channel function under physiological conditions. In the case of $Ca^{2+}$ channels, high-affinity binding sites allow the channel to exclude monovalent cations and to conduct $Ca^{2+}$, $Ba^{2+}$, and $Sr^{2+}$. A similar amino acid region, in the channel outer mouth, underlies the shared open-channel properties of $Ca^{2+}$ channels and cyclic nucleotide-gated channels. In both cases, divalent cation binding is mediated by a set of glutamate (E or Glu) residues (Fig. 1). Four glutamate residues, one from each of the homologous repeats of $Ca^{2+}$ channels, apparently form a cluster of carboxyl groups that is capable of binding at least one divalent cation. Although it is agreed that the four Glu residues do not contribute equally to $Ca^{2+}$ or $Cd^{+}$ binding (Yang et al., 1993; Kim et al., 1993; Tang et al., 1993), it is not clear yet which glutamate residue is more critical for cation permeation. Neutralization of Glu in repeat II with E736Q was shown to have a rather modest effect on channel selectivity and permeation (Yatani et al., 1994; Parent et al., 1995a). Neutralization of Glu in repeat III with E1145Q resulted in a 20-fold decrease in the channel affinity for $Ca^{2+}$ without affecting its single-channel conductance of 22 pS, as measured in the presence of 115 mM $BaCl_2$. In contrast, neutralization of glutamate residue E1446 in repeat IV significantly decreased $Ca^{2+}$ affinity by ≈10-fold and the $Ba^{2+}$ single-channel conductance from 22 to 11 pS. Mutations of E1446 further indicated that steric hindrance influences monovalent cation conductance, with smaller residues yielding higher single-channel conductance. Permeation for divalent cations is more complex, with contributions from both size and charge of the side chain. Maximum divalent conductance could thus be achieved either with small neutral residues such as glycine or else with large negatively charged residues such as glutamate and aspartate. Altogether our results are consistent with a set of at least two high-affinity binding sites located close to the external mouth of the channel, as suggested by Kuo and Hess (1993a,b). Moreover, it is suggested that glutamate residue E1446 in repeat IV is located in the narrow region of the calcium channel outer mouth. Some of these results were presented earlier (Parent et al., 1995a).

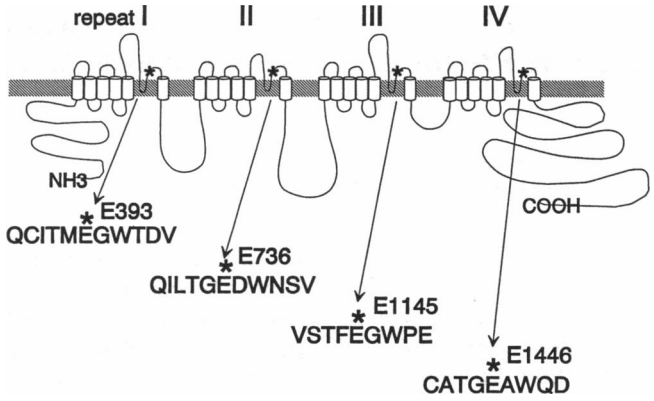


FIGURE 1 Putative model of the secondary structure of the cardiac $\alpha_{1C}$ subunit. $Ca^{2+}$ channels contain four units of repeats labeled I to IV. Each repeat is itself composed of six transmembrane regions and contains a SS1-SS2 region analogous to that of $K^{+}$ channels. The approximate location of glutamate residues E393 in repeat I, E736 in repeat II, E1145 in repeat III, and E1446 in repeat IV targeted in this study are shown by asterisks (*). The sequences of amino acids surrounding the glutamate residues in each repeat are shown below.

## MATERIALS AND METHODS

### Site-directed mutagenesis of the cardiac calcium channel $\alpha_{1C}$ subunit

Standard methods of plasmid DNA preparation and DNA sequencing were used (Sambrook et al., 1989). The wild-type, full-length $\alpha_{1C\text{-}a}$ subunit cDNA (Genbank accession number X15539) was cloned from rabbit heart (Perez-Reyes et al., 1990) and was found to be essentially identical to the sequence published by Mikami et al., (1989). The full-length rabbit $\alpha_{1C}$ was engineered in the pGEM-3 vector (Promega, Madison, WI). Point mutations were performed either by polymerase chain reaction or by subcloning the appropriate DNA fragments into M13 bacteriophage vectors mp 18 and mp 19 followed by oligonucleotide-directed in vitro mutagenesis of the single-stranded template, using the mutagenesis Am-

ersham system V 2.1 (Arlington Heights, IL). The mutated fragments were then subcloned into the full-length cDNA between the following restriction sites: *Sfi*I (271)/*Sfi*I (1567) for mutations E393Q and D397N in repeat I; *Stu*I (1834)/*Bfr*I (2693) for mutations E736Q in repeat II; *Bfr*I (2693)/*Ksp*I (4116) for mutations E1145Q, E1145D, E1145K, E1149K, and E1149D; and *Ksp*I (4116)/*BstE*II (4646) or *Ksp*I (6610) for mutations E1446Q, E1446A, E1446G, E1446D, and D1450N. Constructs were verified by restriction mapping, and the nucleotide sequence of the mutated region was determined by the dideoxy chain termination method using either single- or double-stranded plasmid DNA. The deleted ΔC1733 and ΔNΔC version of wild-type and mutant $\alpha_{1C}$ subunit was used alternatively in some experiments (Wei et al., 1994a,b). The deleted form ΔC1733 construct of the $\alpha_{1C}$ subunit generates barium currents four- to sixfold greater than the full-length wild-type $\alpha_{1C}$, without affecting its single-channel conductance and pharmacological profile (Wei et al., 1994a). Deletion of the first 60 amino acids was also found to produce larger whole-cell barium currents. This current increase was associated with a similar increase in gating currents, without a change in single-channel conductance; thus N-terminus deletion probably improved protein expression (Wei et al., 1994b). With this deletion, the N-terminus of the rabbit $\alpha_{1C}$ subunit (Mikami et al., 1989) becomes identical to the N-terminus of the human $\alpha_{1C}$ (Schultz et al., 1993). In our hands, the double deleted construct ΔNΔC generates whole-cell barium currents 1–2 μA in the absence of dihydropyridine agonist. DNA constructs were linearized at the 3′ end by *Hind III* digestion, and run-off transcripts were prepared using methylated cap analog $m^7G(5')ppp(5')G$ and T7 RNA polymerase (Ambion, Austin, TX).

## Expression of $\alpha_{1C}$ wild-type and mutants in *Xenopus* oocytes

Stage V or VI individual oocytes free of follicular cells were obtained after collagenase treatment (Gibco, Grand Island, NY) (Parent et al., 1995b). cRNA (46 nl) was injected at a concentration of 100 ng/μl for a total of 4.6 ng per oocyte. In some experiments, the $\alpha_1$ subunit was co-injected with auxiliary subunits, brain $\alpha_{2b}$ (generous gift of Dr. Michel de Waard, University of Iowa, Iowa City, Iowa), and cardiac $\beta_{2a}$ (Perez-Reyes et al., 1992) in a 1:1:1 ratio. Oocytes were cultured at 19°C for 3–7 days in the following saline medium: 100 mM NaCl, 2 mM KCl, 1.8 mM $CaCl_2$, 1 mM $MgCl_2$, 5 mM HEPES, 2.5 mM pyruvic acid, and 50 μg/ml gentamicin, pH 7.6.

## Electrophysiological recordings

Whole-cell currents were measured at room temperature with a two-electrode voltage-clamp amplifier (OC-725, Warner Instruments, Hamden, CT). All experiments were performed at room temperature. Voltage and current electrodes (1–2 MW tip resistance) were filled with 3 M KCl, 1 mM EGTA, and 10 mM HEPES (pH 7.4). Oocytes were first impaled in a modified Ringer solution: 96 mM NaOH, 2 mM KOH, 1.8 mM $CaCl_2$, 1 mM $MgCl_2$, and 10 mM HEPES titrated to pH 7.4 with methane sulfonic acid; the bath solution was then exchanged with the appropriate test solution. Oocytes were superfused by gravity flow at a rate of 10 ml/min. Capacitive transients and leak currents were subtracted using the residual currents measured in the presence of 1 mM $CoCl_2$. PClamp software Clampex 5.51 (Axon Instruments, Foster City, CA) was used for on-line data acquisition. Data were sampled at 4 kHz.

Wild-type and mutant channel affinity for calcium ions was assessed from the calcium block of whole-cell $Li^+$ currents. Whole-cell current-voltage (I-V) curve was first measured in the presence of the nominally calcium-free $Li^+$ solution: 120 mM LiOH, 5 mM EGTA, 2 mM KOH, 0.5 mM niflumic acid, and 10 mM HEPES titrated to pH 7.3 with methane sulfonic acid. $Ca(OH)_2$ was added to the solution to obtain the desired level of free calcium. The stability constants used to calculate the free calcium concentration were taken from Fabiato and Fabiato (1979). Calcium block was measured in the absence of dihydropyridine agonist at the peak current, which was found between −20 and −10 mV in most cases, in the presence of auxiliary subunits $\alpha_2$ and $\beta_2$. Concentration-response curves were constructed from measurements of peak inward $Li^+$ currents and 90 s after changing the bath solution to a different $Ca^{2+}$ concentration. The experimental protocol included seven $Li^+$ solutions ranging from 10 nM to 10 mM free-$Ca^{2+}$ and was completed within 15 min. $Ca^{2+}$ block was reversible at 90% in all experiments reported here. Some batches of oocytes were shown to display a higher current run-down and were discarded from the data pool. The current amplitude relative to the control value was plotted against pCa ($-\log [Ca^{2+}]_o$). All data collected for each calcium concentration were pooled and reported as the mean ± SEM. The mean curves were then fitted to the sum of two Hill equations:

$$\frac{I}{I_{max}} = \frac{I_1}{1 + \frac{[Ca^{2+}]}{K_{D1}}} + \frac{I_2}{1 + \frac{[Ca^{2+}]}{K_{D2}}} \quad (1)$$

where $I$ is the peak $Li^+$ current measured at a given $Ca^{2+}$ concentration, $I_{max}$ is the peak current measured in nominally calcium-free $Li^+$ solutions, and $[Ca^{2+}]$ is the free calcium concentration. $I_1$ and $I_2$ are the fractional currents of the two components where $I_1 + I_2 = 1$; $K_{D1}$ and $K_{D2}$ are the apparent dissociation constants. For comparison purposes, $K_{D1}$ is always referred to as the dominant dissociation constant where $I_1 > I_2$.

Single channels were recorded in the cell-attached configuration with an Axopatch 1B patch-clamp amplifier (Axon Instruments) after removing the oocyte vitelline membrane using a hypertonic sucrose solution, as explained previously (Parent et al., 1995b). Patch pipettes (Corning 7052) were coated with Sylgard 184 (Corning Dow, Corning, NY) and fire-polished before use. Oocytes were bathed in an iso-K solution consisting of 140 mM K-Aspartate, 10 mM EGTA, 5 mM $MgCl_2$, and 10 mM HEPES, pH 7.4, to zero membrane potential. Single channels were recorded in the presence of 1 μM (±) Bay K 8644 (Calbiochem, LaJolla, CA) in the patch pipette to promote long channel openings (10–20 ms). Barium single-channel conductance was measured with a pipette solution consisting of 115 mM $BaCl_2$, 1 mM EGTA, and 10 mM Hepes, pH adjusted to 7.4 with *N*-methyl-D-glucamine. In the presence of 1 μM BayK, barium single-channel currents usually activated at ≈−20 mV. Under these conditions, $Ba^{2+}$ currents through the endogenous stretch cation permeable channel (Yang and Sachs, 1989) reversed at Vm ≈+20 mV, whereas $Ba^{2+}$ currents through $\alpha_{1C}$ reversed at Vm > 60 mV.

Single-channel conductance for $Li^+$ was measured with a pipette solution consisting of 120 mM LiCl, 5 mM EGTA, 5 mM TEA-Cl, 0.5 mM niflumic acid, and 10 mM HEPES titrated to pH 7.3 with LiOH. $Li^+$ was selected to minimize current fluctuations induced by proton block observed at pH 7.0 in $Na^+$ solutions (Pietrobon et al., 1989; Prod'hom et al., 1989). The absence of measurable proton block in the presence of $Li^+$ and $Ba^{2+}$ as charge carriers is usually explained by higher affinities of these ions for permeation sites in the pore (Prod'hom et al., 1989). Oocytes were also found to seal more easily in the presence of $Li^+$, with seal resistances routinely higher than 20 GΩ. Unitary $Li^+$ currents through wild-type and mutant $\alpha_{1C}$ were distinguished from $Li^+$ currents through the endogenous cation-permeable stretch channel (Yang and Sachs, 1989) by their voltage-dependent activation. In the presence of 1 μM BayK, lithium single-channel currents activated at $V_m$ ≈−50 mV, as was expected from the more negative surface potential experienced in the presence of monovalent cations. Single-channel conductances were obtained from linear regression of steady-state single-channel amplitude measured between −10 and +20 mV for $Ba^{2+}$ currents and between −50 and 0 mV for $Li^+$ currents. As single-channel I-V curves measured in the cell-attached configuration show considerable Goldmann-Hodgkin-Katz rectification in this range of potentials, this estimation yields single-channel conductance values lower than the instantaneous single-channel conductance of 25 ± 0.5 pS ($n$ = 4) obtained for the wild-type $\alpha_{1C}$ subunit from ramps of potentials applied at 1 V/s between −100 and −20 mV (results not shown). Data were sampled at 5 kHz and filtered at 1.5 kHz. Single-channel recordings were analyzed using PClamp (Axon Instruments) and Eppro software. Van der Waals volumes for residues A (Ala), D (Asp), G (Gly), Q (Gln), K (Lys), and E (Glu) were obtained from Creighton (1993). Data were reported as mean ± SEM.

## RESULTS

### Asymmetric contribution of four glutamate residues to high-affinity $Ca^{2+}$ binding

Electrophysiological studies of native L-type $Ca^{2+}$ channels have provided evidence for the existence of high-affinity binding sites in the micromolar range for $Ca^{2+}$ ions (Hess and Tsien, 1984; Lansman et al., 1986). In $Na^+$ channels, substitution of lysine in repeat III and alanine in repeat IV by glutamate conferred $Ca^{2+}$ channel characteristics onto a $Na^+$ channel (Heinemann et al., 1992). This result suggested that negatively charged residues at this position might determine divalent/monovalent cation selectivity. All $\alpha_1$ subunits of voltage-dependent calcium channels possess a strictly conserved glutamate (E) residue in the H5 pore region. The role of negatively charged glutamate residues in determining $Ca^{2+}$ selectivity has been demonstrated before (Yang et al., 1993; Mikala et al., 1993). The following experiments performed in our lab confirmed the previous findings. In the first step, residues E393, E736, E1145, and E1446 in repeats I, II, III, and IV of the L-type $\alpha_{1C}$ subunit were neutralized by replacement of the negatively charged glutamic acid with the neutral residue glutamine. All mutant channels generated whole-cell inward barium and lithium currents, which were shown to be stimulated by the addition of 1 $\mu$M (±) BayK 8644 to the bath. Furthermore, the mutant channels generally expressed larger barium currents than could be generated by endogenous calcium currents stimulated by co-injection of $\alpha_2$ and $\beta_2$ subunits (Lacerda et al., 1994). Both wild-type and mutant $\alpha_{1C}$ subunits carried whole-cell $Ca^{2+}$ currents, albeit with a lower conductance than $Ba^{2+}$ currents. Outward currents carried by internal $K^+$ ions were substantially increased in mutants E1145Q and E1446Q with an accompanying negative shift in the apparent reversal potential. This observation suggests that divalent cation selectivity is reduced in these mutations, although reversal potentials measured under these conditions could not be reliably quantified.

Channel affinity for $Ca^{2+}$ ions was assessed from $Ca^{2+}$ block of whole-cell lithium currents. Whole-cell $Li^+$ currents of wild-type and mutant $Ca^{2+}$ channels are shown before and after the addition of 1 $\mu$M free-$Ca^{2+}$ (Fig. 2). Current traces are shown for full-length wild-type and mutant $\alpha_{1C}$ subunits co-injected with $\alpha_2$ and $\beta_2$, but similar results were obtained with double deleted constructs $\Delta N \Delta C$ in the absence of auxiliary subunits. Currents were elicited by 450-ms depolarizing test potentials applied at a frequency of 0.2 kHz from a holding potential of −60 mV. Block was always measured at the peak current, which was determined before each experiment. Because of the reduced divalent over monovalent selectivity in these mutants, whole-cell currents could only be accurately measured over a narrow range of potentials between −30 and +10 mV.

The bottom right panel shows the complete inhibition curves for the four mutants and the wild-type channel. As seen, data were best fitted by assuming two binding processes with distinct affinities for $Ca^{2+}$ ions (Eq. 1). These two binding sites may reflect the presence of more than one $Ca^{2+}$ ion in the pore, especially at high concentrations, resulting in negative cooperativity as suggested in previous models of $Ca^{2+}$ channel permeation. Table 1 displays the $K_D$ values and their fractional contribution (shown in parentheses) obtained from the least-square fits to Eq. 1 for the inhibition curves in Figs. 2, 3, and 4. As seen in Table 1, the wild-type channel inhibition curve was best fitted by a sum of two binding sites with dissociation constants of 30 nM and 3 $\mu$M. The physical meaning of the nanomolar-affinity binding site is unclear at this time and is currently investigated at the single-channel level. Neutralization of glutamate residue E736 in repeat II had no significant effect on the channel $Ca^{2+}$ affinity, with similar values for $K_{D1}$ and $K_{D2}$. Stronger effects were observed for neutralization of glutamate residues in repeats I, III, and IV. For E393Q in repeat I, the data were best fitted with $K_{D1}$ = 64 nM (0.44) and $K_{D2}$ = 5 $\mu$M (0.56). For E1145Q (repeat III) and E1446Q (repeat IV), the dose-response curves were shifted to the right with higher $K_{D2}$ = 12 $\mu$M (0.65) and $K_{D2}$ = 13

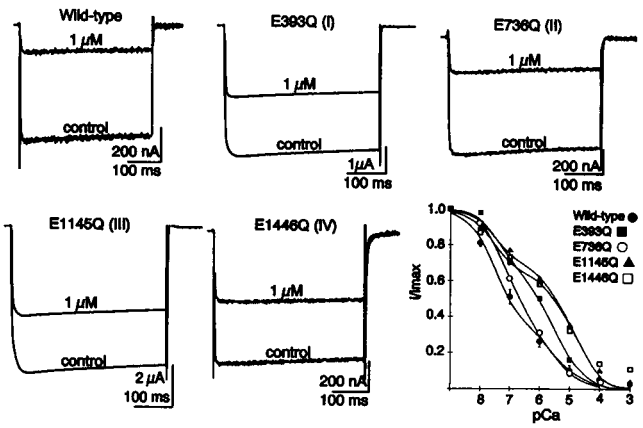


FIGURE 2 Asymmetric contribution of glutamate residues to high-affinity $Ca^{2+}$ binding. Residues E393, E736, E1145, and E1446 in repeats I, II, III, and IV were neutralized by replacement of glutamate by glutamine. Current traces were recorded 4 days after co-injection of wild-type and mutant $\alpha_1$ with equimolar concentration of $\alpha_2$ and $\beta_2$ subunits. Channel affinity for $Ca^{2+}$ ions was assessed from $Ca^{2+}$ block of whole-cell lithium currents. Whole-cell $Li^+$ currents of wild-type and mutant $Ca^{2+}$ channels are shown before and after the addition of 1 $\mu$M free-$Ca^{2+}$. Currents were elicited by 450-ms depolarizing test potentials applied at a frequency of 0.2 kHz from a holding potential of −60 mV. Block was measured at the peak current of −10 mV. Averaged fractional peak currents ± SEM ($n$ = 3) were plotted as a function of the external free $Ca^{2+}$ concentration. The bottom right panel shows the complete inhibition curves for the four mutants and the wild-type channel. Smooth curves are least-squares fits to Eq. 1, and estimated $K_D$s are reported in Table 1. Neutralization of glutamate residues in repeat II (E736Q) had no significant effect on the channel affinity for $Ca^{2+}$. Mutants E393Q (I), E1145Q (III), and E1446Q (IV) were shown to display reduced affinity for $Ca^{2+}$. All these experiments were performed on the same batch of oocytes, which gave peak endogenous calcium currents <50 nA when measured in $Ca^{2+}$-free $Li^+$ solutions. The single-letter codes for amino acids used in our study: A, alanine; G, glycine; E, glutamate; Q, glutamine; D, aspartate; N, asparagine; and K, lysine.

**TABLE 1 Affinities of the wild-type and mutant $\alpha_{1C}$ channels for $Ca^{2+}$ ions**

| Channels | $K_{D1}$ (nM) | $K_{D2}$ ($\mu$M) |
|---|---|---|
| Wild-type | 30 nM (0.66) | 3 $\mu$M (0.34) |
| E393Q | 64 nM (0.44) | 4 $\mu$M (0.56) |
| E736Q | 87 nM (0.71) | 5 $\mu$M (0.29) |
| E1145Q | 40 nM (0.35) | 12 $\mu$M (0.65) |
| E1446Q | 29 nM (0.38) | 13 $\mu$M (0.62) |
| E1145D | 38 nM (0.68) | 3 $\mu$M (0.32) |
| E1145Q | 25 nM (0.24) | 16 $\mu$M (0.77) |
| E1145K | 140 nM (0.33) | 467 $\mu$M (0.67) |
| E1446D | 32 nM (0.55) | 3 $\mu$M (0.45) |
| E1446Q | 64 nM (0.48) | 23 $\mu$M (0.52) |
| E1446A | 180 nM (0.17) | 43 $\mu$M (0.83) |
| E1446G | 120 nM (0.30) | 33 $\mu$M (0.70) |

Inhibition curves obtained from the $Ca^{2+}$ block of peak whole-cell $Li^+$ currents were fitted to a sum of two binding sites (Eq. 1). Under most instances, $Ca^{2+}$ block was measured at $-10$ mV. Estimated $K_{D1}$ and $K_{D2}$ are reported for the wild-type and mutant channels. The fractional currents of the two components $I_1$ and $I_2$ are shown in parentheses. Glutamate substitutions were shown to affect the $Ca^{2+}$ affinity of the second binding site $K_{D2}$.

$\mu$M (0.62) respectively. Neutralization of the glutamate residues in repeats III and IV was shown to significantly affect the micromolar-affinity binding site with little effect on the higher affinity binding site. These data are consistent with the current view that the four glutamate residues do not contribute equally to $Ca^{2+}$ binding (Yang et al., 1993) and further suggest that glutamate residues in repeats III and IV are critical in defining the micromolar-affinity $Ca^{2+}$ binding sites in the channel pore.

The contribution of neighboring negatively charged residues to high-affinity $Ca^{2+}$ binding was also estimated. The cardiac $\alpha_{1C}$ subunit has four additional negatively charged residues in the SS2 region of H5: D397 (I), D737 (II), E1149 (III), and D1450 (IV). D397N, E1149K, and D1450N did not affect high-affinity $Ca^{2+}$ block or single-channel properties (results not shown). In summary, our results are consistent with previous reports that a series of glutamate residues located in the SS2 portion of the pore region specifically contribute to high-affinity $Ca^{2+}$ binding in voltage-dependent calcium channels (Tang et al., 1993; Yatani et al., 1994).

High-affinity $Ca^{2+}$ binding requires negatively charged residues. The nature of interactions controlling divalent cation selectivity in the pore of calcium channels was then examined with a mutational analysis of residue E1145. It has been hypothesized before that high-affinity $Ca^{2+}$ binding in the calcium channel pore is achieved through coordination with oxygen donor groups (Lansman, 1990). Results shown in Fig. 2 strongly suggest that the carbonyl (C = O) groups of glutamine residues may not provide sufficient interaction with $Ca^{2+}$ and that negatively charged carboxylate groups are required to achieve affinity in the $\approx$0.1 $\mu$M range. The following mutations were thus designed to address the importance of negatively charged residues at the high-affinity binding site. Fig. 3 shows the calcium block of whole-cell $Li^+$ currents for mutations E1145D (conservation of the carboxylate group), E1145Q (charge neutralization), and E1145K (substitution with a positively charged residue). The dose-response curves were best fitted by a sum of two binding sites with the micromolar dissociation constant $K_{D2}$ clearly the most affected by charge substitutions. Conservation of the negative charge with mutation E1145D preserved $Ca^{2+}$ high-affinity binding; the $K_{D1}$ and $K_{D2}$ values obtained from the fit were virtually identical to the fit parameters obtained for the

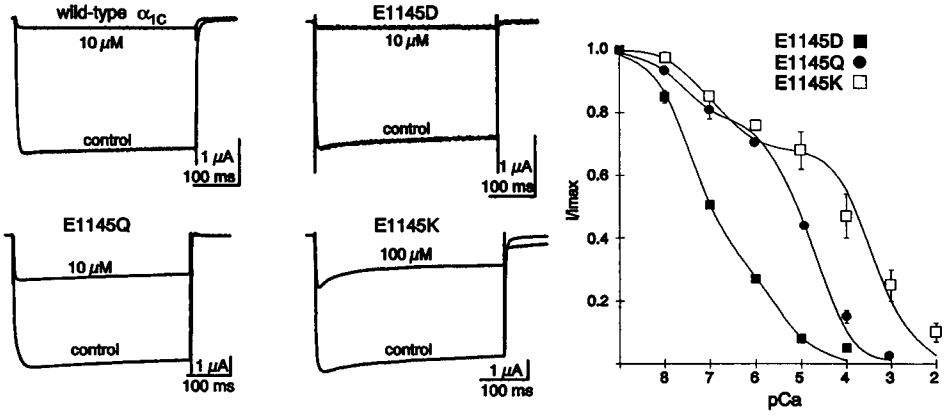


FIGURE 3 Functional equivalence of negatively charged residues. Whole-cell $Li^+$ currents of wild-type and mutants E1145D, E1145Q, and E1145K are shown before and after the addition of 10 or 100 $\mu$M free $Ca^{2+}$ to the bath. The right panel shows the corresponding inhibition curves. Each data point is the mean fractional peak current ($n$ = 3) plotted as a function of the external $Ca^{2+}$. SEM was smaller than the symbols in all cases. Smooth curves are the least-squares fits to Eq. 1. Estimated $K_D$ values are reported in Table 1. Calcium affinity was found to be strongly influenced by the net charge of the residue. Charge conservation in E1145D preserved high-affinity $Ca^{2+}$ binding with a dose-response curve virtually identical to the wild-type channel. Although charge neutralization in E1145Q significantly decreased $Ca^{2+}$ affinity, lysine substitution at this position virtually abolished $Ca^{2+}$ selectivity. In this series of experiments, wild-type and mutant $\alpha_1$ were co-injected with auxiliary subunits $\alpha_2$ and $\beta_2$. Experiments shown here were conducted with oocytes coming from the same frog donor, which gave consistent peak endogenous $Li^+$ currents <60 nA.

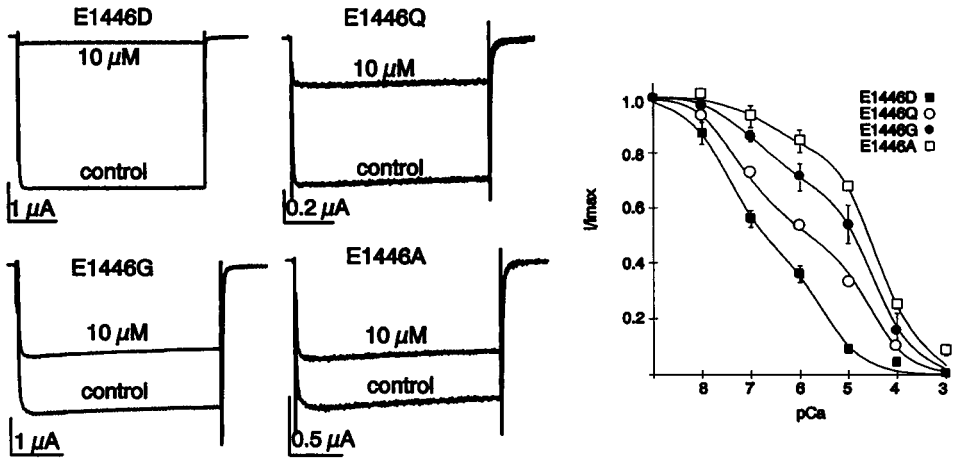


FIGURE 4 Mutational analysis was conducted at position 1446 in repeat IV to assess the nature of interactions at the $Ca^{2+}$ binding site. Mutant $\alpha_1$ subunits were co-injected with auxiliary subunits $\alpha_2$ and $\beta_2$. Whole-cell $Li^+$ currents are shown for mutants E1446D, E1446Q, E1446G, and E1446A before and after the addition of 10 $\mu$M free-$Ca^{2+}$. The right panel shows the corresponding inhibition curves. Each data point represents the averaged fractional peak current ($n$ = 4) measured for each free $Ca^{2+}$. The smooth lines connecting data points are the least-squares fits to Eq. 1. Corresponding $K_D$ values are reported in Table 1. As seen in repeat III, conservation of the negative charge E1446D preserved $Ca^{2+}$ micromolar-affinity binding. Although neutralization of the negative charge with size conservation in E1446Q significantly decreased $Ca^{2+}$ affinity, substitution by smaller hydrophobic residues alanine and glycine further reduced the channel affinity, with $K_{D2}$ = 43 $\mu$M for E1446A and $K_{D2}$ = 33 $\mu$M for E1446G. Horizontal scale bars are 100 ms throughout.

wild-type channel (Table 1). Although $Ca^{2+}$ affinity was significantly reduced in mutant E1145Q ($K_{D2}$ = 16 $\mu$M), replacing the glutamate residue by the positively charged lysine residue shifted the inhibition curve by three orders of magnitude, essentially abolishing $Ca^{2+}$ affinity with a calculated $K_{D2}$ = 467 $\mu$M (Table 1). Furthermore, no inward whole-cell $Ba^{2+}$ current was ever recorded with the E1145K mutant, suggesting that divalent cations may not permeate through the mutant channel. Results with the glutamate mutants in pore III suggest that negative carboxylate groups are required for $Ca^{2+}$ binding. Furthermore the size difference between the glutamate and the aspartate

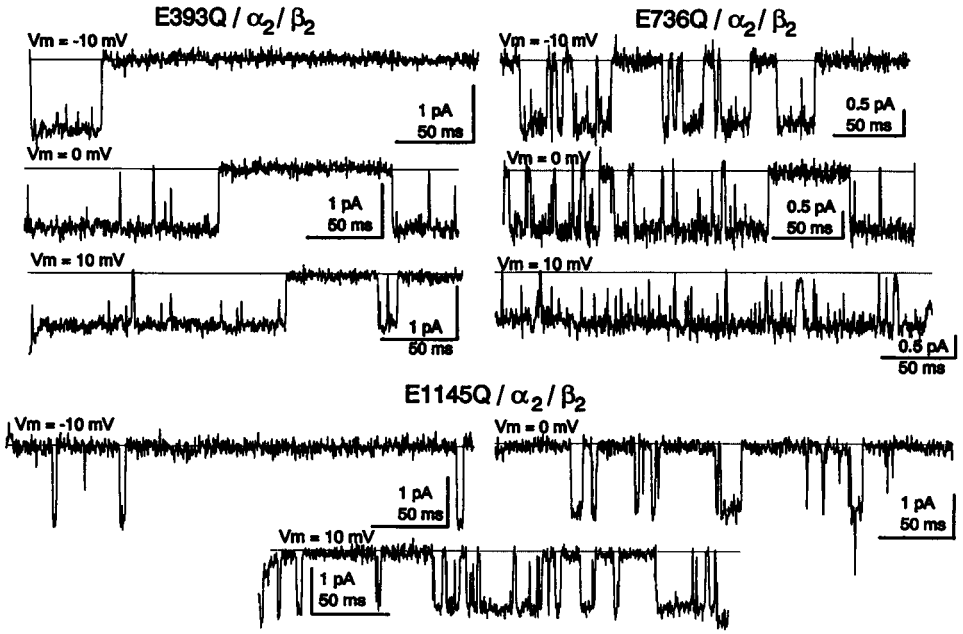


FIGURE 5 Single-channel properties of E393Q, E736Q, and E1145Q co-injected with auxiliary subunits $\alpha_2$ and $\beta_2$. Single channels were recorded in the cell-attached configuration in the presence of an isotonic $K^+$ bath. Patch pipettes were filled with 115 mM $BaCl_2$ and 1 $\mu$M BayK. Single channels were elicited by 400-ms depolarization steps to −10, 0, and 10 mV from a holding potential of −80 mV. E393Q, E736Q, and E1145Q showed little differences in the single-channel properties. Furthermore, there was no noticeable change in the single-channel conductance of 22 pS (see Fig. 6 for mean I-V curves), with a mean current of −1.2 pA at 0 mV. This result argues that E393, E736, and E1145 are not critical for permeation in calcium channels.

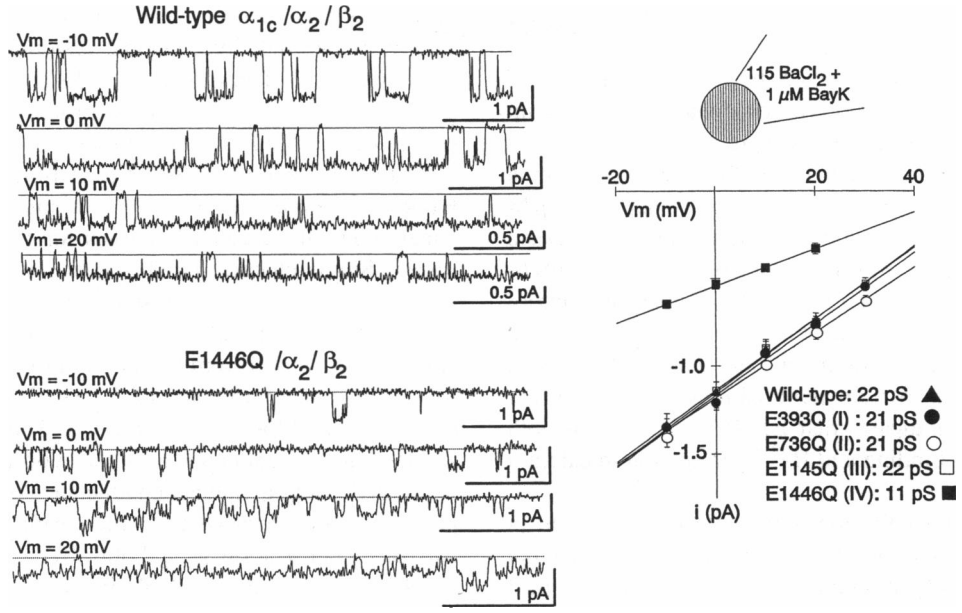


FIGURE 6 Single-channel properties of wild-type and mutant E1446Q in repeat IV. Single channels were recorded in the cell-attached configuration in the presence of an isotonic $K^+$ bath. Patch pipettes were filled with 115 mM $BaCl_2$ and 1 μM BayK. Single channels were elicited by 400-ms depolarization steps to −10, 0, 10, and 20 mV from a holding potential of −80 mV at a frequency of 0.5 kHz. Single-channel conductance was significantly decreased from 22 pS for the wild-type to 11 pS for E1446Q. This result argues that E1446 is critical for both high-affinity $Ca^{2+}$ binding and $Ba^{2+}$ permeation in calcium channels. Scale bars are 1 pA and 50 ms throughout. The right panel shows the corresponding mean I-V curves for the wild-type and mutant channels from a minimum of three different oocytes. Single-channel conductance was obtained from linear regression of steady-state single-channel amplitude measured between −10 and +20 mV.

residue ($-CH_2$) does not significantly affect $Ca^{2+}$ affinity, which suggests that charge effects are especially critical and may dominate over steric effects at the $Ca^{2+}$ ligand site.

The role of electrostatic and steric hindrance mechanisms in $Ca^{2+}$ binding was further addressed by side-chain substitution of E1446 in repeat IV. Fig. 4 shows typical whole-cell $Li^+$ currents recorded for mutants E1446D, E1446Q, E1446G, and E1446A before and after the addition of 10 μM free-$Ca^{2+}$. As expected, conservation of the negative charge in E1446D preserved high-affinity $Ca^{2+}$ binding (Table 1), which indicates that electrostatic interactions dominate size effects at the ligand site. Although neutralization of the negative charge with size conservation in E1446Q significantly altered $Ca^{2+}$ affinity, substitution by smaller neutral hydrophobic residues alanine and glycine had stronger effects, decreasing $Ca^{2+}$ affinity with $K_{D2}$ = 43 μM (E1446A, $n$ = 4) and $K_{D2}$ = 33 μM (E1446G, $n$ = 3) (Table 1). These results indicate that negatively charged residues such as glutamate and aspartate are essential for high-affinity $Ca^{2+}$ binding but that neutral hydrophilic with oxygen donor groups such as glutamine can achieve moderate affinity. Small neutral hydrophobic residues like alanine and glycine are almost as ineffective as the positively charged lysine residue in selecting $Ca^{2+}$ in a monovalent solution. Sensitivity of $Ca^{2+}$ block to the chemical nature of these residues suggests that $Ca^{2+}$ contacts the channel at this region of its molecular surface.

$Ba^{2+}$ single-channel conductance is modified by E1446 mutation in repeat IV. It is generally agreed that high-affinity $Ca^{2+}$ binding sites are located in the permeation pathway in proximity to the external mouth of the channel (Tsien et al., 1987; Armstrong and Neyton, 1992; Kuo and Hess, 1993a,b). Changes in $Ca^{2+}$ affinity are thus expected to alter divalent cation permeation. Single-channel recordings of glutamate mutants in repeats I, II, and III are shown in Fig. 5. Patch pipettes were filled with 115 mM $BaCl_2$. Single channels were elicited by 400-ms depolarization steps to −10, 0, and 10 mV from a holding potential of −80 mV in the presence of 1 μM BayK. Mutations E393Q, E736Q, and E1145Q showed few differences in the single-channel properties, including voltage-dependent open channel probability and open time distribution, suggesting that gating properties were not significantly altered. Furthermore, the single-channel conductance was not affected with a mean current of −1.2 ± 0.15 pA ($n$ = 20) at 0 mV for mutants E393Q, E736Q, and E1145Q (see mean I-V curve in Fig. 6). Because single-channel I-V curves measured in the cell-attached configuration showed considerable Goldmann-Hodgkin-Katz rectification in this range of potentials, this estimation yields single-channel conductance values lower than the instantaneous single-channel conductance of 25 ± 0.5 pS ($n$ = 4) obtained from ramps of potentials applied at 1 V/s between −100 and −20 mV (results not shown). The mean single-channel conductance was 21 ± 2 pS for E393Q ($n$ = 3), 22 ± 1 pS for E736Q ($n$ = 3), and 22 ± 2 pS for E1145Q ($n$ = 3). This suggests that although residues E393, E736, and E1145 actively participate in

$Ca^{2+}$ binding, none of these residues is rate-limiting for permeation in calcium channels.

Single-channels events carried by 115 mM $Ba^{2+}$ are shown in Fig. 6 for the wild-type $\alpha_{1C}$ channel and mutant E1446Q. Again, single channels were elicited by 400-ms depolarization steps to −10, 0, 10, and 20 mV from a holding potential of −80 mV in the presence of 1 μM BayK. Single-channel conductance significantly decreased from 22 ± 0.5 pS ($n$ = 6) for the wild-type to 11 ± 1 pS ($n$ = 12) for mutation E1446Q. A reduction of the single-channel conductance at the same position was also observed for the human $\alpha_{1C}$ E1387Q mutant and was attributed to a weaker competition for divalent cations (Yatani et al., 1994). This result indicates that E1446 is critical for both high-affinity $Ca^{2+}$ binding and $Ba^{2+}$ permeation in calcium channels.

At high $Ba^{2+}$ concentration, glutamate neutralization in repeats I, II, and III did not change the single-channel conductance. In contrast, glutamate neutralization in repeat IV with E1446Q was found to specifically decrease the single-channel conductance to 11 pS from a conductance of 22 pS for the wild-type $\alpha_{1C}$ channel.

Mutations of E1446 affect both monovalent and divalent cation single-channel conductance. Mutations of glutamate E1446 in repeat IV were further shown to alter divalent and monovalent cation single-channel conductance. Negative residues at this position were shown to confer higher $Ca^{2+}$ affinity than small hydrophobic residues (see Fig. 4). To investigate the effect of charge and size on channel permeation, single channels were recorded with $Ba^{2+}$ as the charge carrier for E1446D, E1446G, and E1446A. Typical recordings are shown in Fig. 7 for E1446G (*top panel*) and E1446A (*bottom panel*) at −10, 0, and 10 mV. The right panel shows the mean I-V curves for these corresponding traces. Single-channel conductances were obtained from linear regression of steady-state single-channel amplitude measured between −10 and +20 mV. $Ba^{2+}$ single-channel conductance varied from a minimum of 11 ± 1 pS ($n$ = 7) for E1446Q to a maximum of 22 pS. E1446D (22 ± 1 pS, $n$ = 3) and E1446G (21 ± 2 pS, $n$ = 3) displayed the same single-channel conductance as the wild-type $\alpha_{1C}$ channel, whereas the single-channel conductance of E1446A (18 ± 2 pS, $n$ = 7) was somewhat smaller. Although $Ca^{2+}$ affinity and $Ba^{2+}$ permeation were both affected by mutations of E1446, there was not a simple inverse correlation between $Ca^{2+}$ affinity and divalent conductance. The sequence of $Ca^{2+}$ affinity with E1446A ≈ E1446G < E1446Q < E1446D ≈ E1446 would have predicted a smaller single-channel conductance for E1446G than for E1446Q. Instead, the single-channel $Ba^{2+}$ conductance sequence follows E1446Q < E1446A < E1446G ≈ E1446D ≈ E1446. Moreover, the lower $Ca^{2+}$ affinity of mutant channels ver-

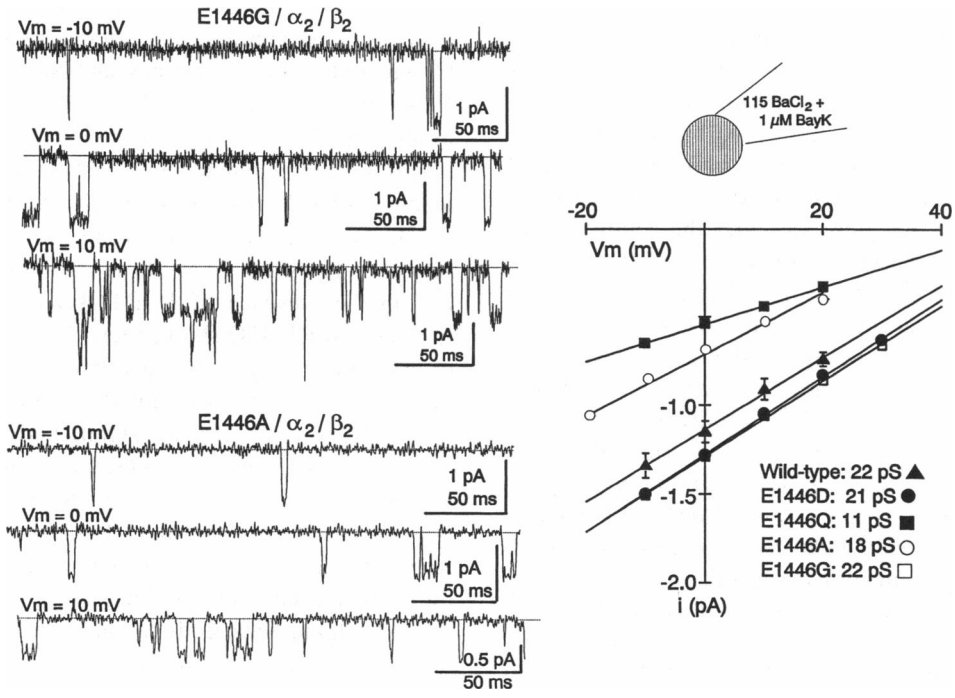


FIGURE 7 Single-channel $Ba^{2+}$ currents for mutants at position 1446 in repeat IV. Single channels were recorded in the cell-attached configuration in the presence of an isotonic $K^+$ bath. Patch pipettes were filled with 115 mM $BaCl_2$ and 1 μM BayK. Single channels were elicited by 400-ms depolarization steps to −10, 0, and 10 mV from a holding potential of −80 mV. Single-channel recordings are shown for E1446G (*top panel*) and E1446A (*bottom panel*). The right panel shows the mean I-V curves obtained for wild-type (▲), E1446D (●), E1446G (□), E1446A (○), and E1446Q (■) from a minimum of three separate patches. Single-channel conductance was obtained from linear regression of steady-state single-channel amplitude measured using amplitude histograms between −10 and +20 mV. $Ba^{2+}$ single-channel conductance varied from 11 to 22 pS. E1446D and E1446G displayed a $Ba^{2+}$ single-channel conductance of 22 pS, not significantly different from the wild-type single-channel conductance.

sus the wild-type channel did not result in larger unitary currents. Single-channel conductance reached plateau at 22 pS for E1446 ≈ E1446D ≈ E1446G. This suggests that although affinity and permeation are determined by a common site and are both influenced by similar factors, steric hindrance plays a major role in divalent cation permeation, whereas $Ca^{2+}$ affinity is determined by the charge or hydrophilicity of the residue. Indeed, as shown in Fig. 9, $Ba^{2+}$ single-channel conductance increased for neutral residues E1446G > E1446A > E1446Q as an inverse function of the volume of the side chain. However, steric hindrance fails to satisfactorily account for the high single-channel conductance of bulkier but negatively charged residues in E1446D and in wild-type E1446. This suggests that electrostatic interactions at the ligand sites are somewhat critical for divalent permeation through the calcium channel pore.

Monovalent cation conductance was also altered by mutations of E1446. This observation was rather unexpected because monovalent cations are more loosely bound and presumably do not depend on strong ion-ion interactions to diffuse through the pore. Single channels were recorded in the cell-attached configuration in the presence of an isotonic $K^+$ bath. Patch pipettes were filled with 120 mM LiCl and 5 mM EGTA. Single channels were elicited by 400-ms depolarization steps to −50, −40, −30, and −20 mV from a holding potential of −80 mV in the presence of 1 μM BayK. $Li^+$ single- channel recordings are shown in Fig. 8 for wild-type (*upper left panel*), E1446Q (*upper middle panel*), E1446D (*lower left panel*), and E1446G (*lower middle panel*). The right panel shows the mean I-V curves, each one obtained from a minimum of three separate experiments. Wild-type $Li^+$ single-channel conductance was 26 ± 1 pS, as measured from linear regression of steady-state single-channel amplitudes between −50 and 0 mV. Single-channel conductance increased to 37 ± 2 pS ($n$ = 3) for E1446A and to 40 ± 3 pS ($n$ = 3) for E1446G, whereas single-channel conductance of 25 ± 1 pS ($n$ = 2) for E1446D and 23 ± 1 pS ($n$ = 3) for E1446Q are not significantly different from the wild-type single-channel conductance. $Li^+$ single-channel conductance was found to be inversely proportional to the side-chain volume (Fig. 9). The calcium channel pore thus seems to behave like a simple molecular sieve in the presence of monovalent cations. This supports the current view that monovalent cations do not tightly bind to a ligand site in the pore; hence electrostatic interaction with charge coordination is not critical for permeation. Altogether, these results demonstrate that E1446 is critical for monovalent and divalent cation diffusion in calcium channels.

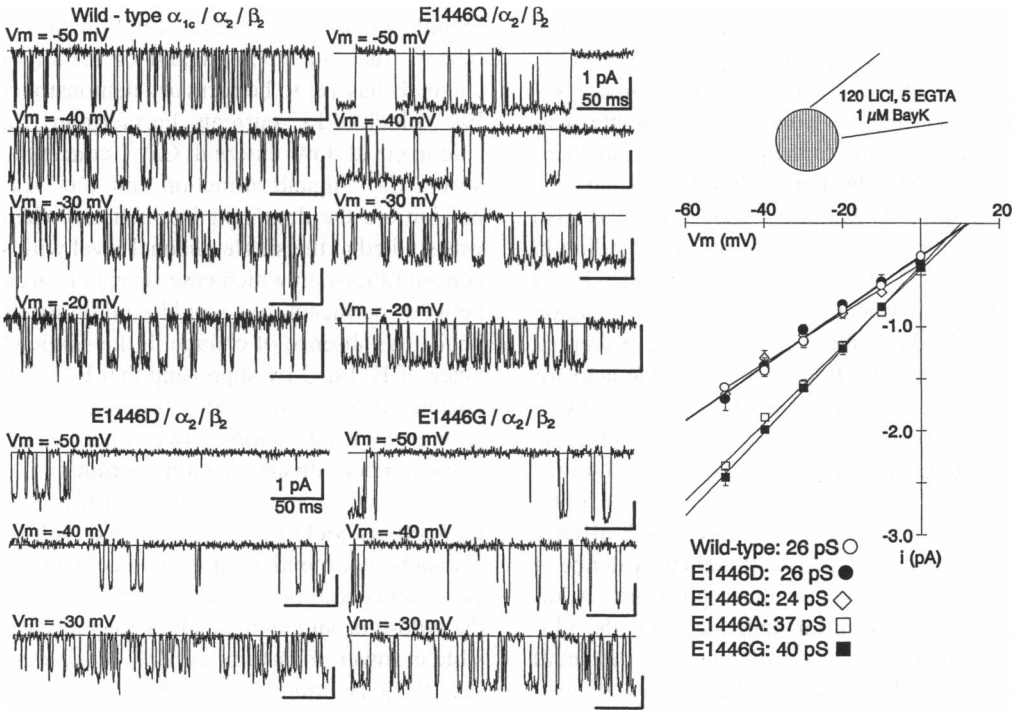


FIGURE 8 Monovalent conductance is affected by mutations at position 1446 in repeat IV. Single channels were recorded in the cell-attached configuration in the presence of an isotonic $K^+$ bath. Patch pipettes were filled with 120 mM LiCl, 5 mM EGTA, and 1 μM BayK. Single channels were elicited by 400-ms depolarization steps to −50, −40, −30, and −20 mV from a holding potential of −80 mV. $Li^+$ single-channel recordings are shown for wild-type (*upper left panel*), E1446Q (*upper middle panel*), E1446D (*lower left panel*), and E1446G (*lower middle panel*). Scale bars are 1 pA and 50 ms throughout. The right panel shows the mean I-V curves. Wild-type $Li^+$ single-channel conductance was estimated to 26 pS from linear regression of steady-state single-channel amplitudes measured between −50 and 0 mV. Single-channel conductance increased to 37 pS for E1446A (□) and to 40 pS for E1446G (■), whereas the single-channel conductance for E1446D (●) and E1446Q (◇) were not significantly different from the wild-type (○) single-channel conductance of 26 pS.

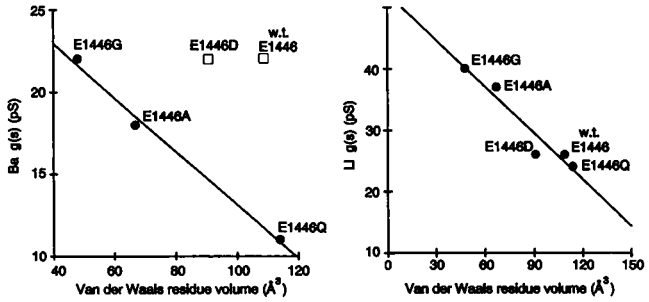


FIGURE 9 Single-channel conductance (*left*) measured with $Ba^{2+}$ as the charge carrier for mutants at position 1446 is shown as a function of the volume of the residue. Size correctly predicts single-channel conductance for neutral residues (alanine, glycine, and glutamine) but underestimates the single-channel conductance of negatively charged aspartate and glutamate residues. $Li^+$ single-channel conductance (*right*) was found to be inversely proportional to the size of the side-chain substitution. Monovalent cation conductance seems to be determined by steric hindrance for all residues at this position, hence the pore behaves like a molecular sieve. Altogether, these results suggest that E1446 is located in the narrow region of the calcium channel pore.

## DISCUSSION

In the present study, we have examined the functional role of the highly conserved glutamate residues located in the SS2 region of repeats I, II, III, and IV of the cardiac $\alpha_{1C}$ subunit. Our results demonstrate that substitution of the glutamic acid residue with glutamine reduced $Ca^{2+}$ affinity in the following order: wild-type $\geq$ EIIQ > EIQ > EIVQ $\geq$ EIIIQ. These results qualitatively agree with previous studies, which have shown that the conserved glutamate residues contribute asymmetrically to the pore of calcium channels (Yang et al., 1993; Mikala et al., 1993). Consistent with our results, the glutamate residue in repeat III was also found to be highly critical for high-affinity $Ca^{2+}$ binding in $\alpha_{1C}$ (Yang et al., 1993) and in $\alpha_{1A}$ (Kim et al., 1993) calcium channels. Mutational analysis at this position showed that conservation of the negative charge preserved $Ca^{2+}$ affinity and that substitution of the glutamic acid for the positively charged lysine decreased $Ca^{2+}$ affinity by $\approx$ 1000-fold, suggesting that a strong electrostatic interaction is required at the ligand site. Negative charge substitutions at E1446 in repeat IV likewise preserved $Ca^{2+}$ affinity. Carboxylate groups are critical to achieve high-affinity $Ca^{2+}$ binding, as suggested by the functional equivalence of glutamate and aspartate residues at these positions. Additional substitutions at this position indicated that the glutamine residue achieved higher $Ca^{2+}$ affinity than did small neutral hydrophobic residues such as alanine and glycine. This is not surprising given the fact that glutamine is a polar residue that contributes to $Ca^{2+}$ ligand sites in other proteins (DaSilva and Williams, 1993). Altogether, our results indicate that the $Ca^{2+}$ binding process probably involves electrostatic interactions with anionic groups acting as the choice coordinating ligands and with large hydrophilic oxygen donor residues contributing somewhat to a reduced $Ca^{2+}$ binding. Our results infer that two glutamate residues, E1145 and E1446, play a dominant role in controlling divalent over monovalent cation selectivity in calcium channels. These residues could thus account for the two high-affinity $Ca^{2+}$ binding sites located in proximity to the external mouth of the pore predicted by Kuo and Hess (1993a,b).

In the classical model of calcium channel permeation, electric repulsion between cations at the high-affinity $Ca^{2+}$ binding site is expected to control the rate of divalent cation diffusion through the channel (Hess et al., 1986; Tsien et al., 1987). In native cardiac cells, the permeability ratio of permeant ions ($Ca^{2+}$, $Sr^{2+}$, $Ba^{2+}$, $Li^+$, $Na^+$, $K^+$) was found to be inversely related to the flux rate, as if high-affinity binding decreases ion mobility (Tsien et al., 1987). Mutations that reduce $Ca^{2+}$ affinity are thus expected to show altered cation permeation. Neutralization of the conserved glutamate residue by substitution of the anionic carboxylate group by a neutral carbonyl group failed, however, to significantly alter the unitary current amplitude carried by saturating $Ba^{2+}$ for mutations E393Q (I), E736Q (II), and E1145Q (III). This observation is easily compatible with the small reduction in $Ca^{2+}$ affinity observed for E393Q (I) and E736Q (II). However, the mutation E1145Q showed no change in its single-channel conductance and showed a significant decrease in its $Ca^{2+}$ affinity. At this time, it cannot be ruled out that changes in $Ca^{2+}$ affinity may not necessarily translate to changes in $Ba^{2+}$ conductance. Although widely used, the assumption that $Ca^{2+}$ and $Ba^{2+}$ bind to the same pore ligand or affinity site in calcium channels has yet to be formally demonstrated by measuring $Ba^{2+}$ block of $Li^+$ currents. Furthermore, $Ca^{2+}$ affinity was examined at low external $Ca^{2+}$ concentrations at which strong $Ca^{2+}$-ligand attraction and $Ca^{2+}$-$Li^+$ moderate repulsion are the dominant interactions, whereas permeation was studied at the single-channel level with saturating $Ba^{2+}$ concentrations, in which case strong electrostatic repulsions between permeant ions would predominate. One could reconcile the absence of change in the single-channel conductance of E1145Q by supposing that E1145 is located in the channel outer mouth. At saturating $Ba^{2+}$ concentrations, strong repulsion factors between permeant ions could prevail upon poor divalent cation coordination at the ligand site and succeed in speeding up ion diffusion. Strong ion-ion interactions could better be achieved with E1145 facing the channel outer mouth in direct contact with high extracellular $Ba^{2+}$ concentration. In such an environment, deviation from the wild-type single-channel conductance could still be possible at lower nonsaturating $Ba^{2+}$ concentrations (Sather et al., 1995). Neutralization of the glutamate residue in repeat IV with E1446Q was shown to notably reduce the $Ba^{2+}$ single-channel conductance from 22 to 11 pS. In this case, ion-ion interactions might not be strong enough to overcome the weak divalent cation coordination at the ligand site, and $Ba^{2+}$ would diffuse rather slowly. This could suggest that the glutamate residue E1446 (IV) may not be as accessible as glutamate residue E1145 (III) from the extracellular medium. This interpretation departs from previous

reports that identified E1446 (IV) as the outermost glutamate residue in the calcium channel pore (Yang et al., 1993). Indeed, results obtained by two independent groups pointed out E1446K as the only E → K mutant to produce ≈200 nA of inward $Ba^{2+}$ whole-cell currents (Yang et al., 1993; Mikala et al., 1993), suggesting that side-chain substitution at this position in pore IV does not critically influence divalent permeation. On the other hand, glutamate substitution by glutamine in E1446Q (IV) was found to produce unitary currents with a reduced $Ba^{2+}$ single-channel conductance (this work; Yatani et al., 1994). It can be argued that the nature of the side chain (lysine versus glutamine) is itself responsible for the differences in the results. Thus the determination of the glutamate residue orientation within the pore will await the development of specific structural probes.

Mutation E1446D, which preserves the net negative charge and high-affinity $Ca^{2+}$ binding in the channel pore, was shown to carry $Ba^{2+}$ with the same single-channel conductance as the wild-type channel. In the absence of strong coordination provided by anionic groups at this binding site, $Ba^{2+}$ permeation was shown to become remarkably sensitive to steric hindrance. Results with glutamine, alanine, and glycine substitution at position 1446 showed that the smallest neutral residues can promote the highest single-channel conductance. In fact, steric effects are strongly competing with electrostatic interaction at the high-affinity site during permeation, as the results obtained with E1446G illustrated. E1446G achieved the $Ba^{2+}$ single-channel conductance of the wild-type channel despite a 100-fold decrease in $Ca^{2+}$ affinity.

Monovalent cations do not bind to the pore high-affinity well as strongly as divalent cations do, and they do not experience ion-ion repulsion effects as strongly, hence their permeation should not be as sensitive to the net charge carried by the ligand site. Substitutions at the position E1446 were used to explore this postulate. Single-channel conductance was measured in the presence of $Li^+$ as the charge carrier to circumvent the prevalent proton block observed at physiological pH in $Na^+$ solutions (Pietrobon et al., 1989). In the presence of $Li^+$ as the charge carrier, there was little difference between the single-channel conductance generated by the negative glutamate and the neutral residue glutamine. However, substitutions by the small neutral residues alanine and glycine resulted in a significantly increased single-channel conductance from 26 pS for the wild-type channel to 37 pS for E1446A and 40 pS for E1446G. The increase in single-channel conductance with smaller residues is compatible with the prevalence of steric effects in the absence of high-affinity ions in the pore. Monovalent single-channel conductance thus seemed to be strictly determined by the size of the residue, independent of its charge. This observation mirrors previous reports that the permeability of monovalent cations in native calcium channels is determined mainly by the cation size (McCleskey and Almers, 1985) and that for ions of the same charge, permeability decreases monotonically with increasing ion size (Hess et al., 1986). Both sets of observations support the view that in the absence of a high-affinity divalent cation, calcium channels behave like a simple molecular sieve. Altogether our results are compatible with a different energy profile for divalent and monovalent cations in the calcium channel pore (Tsien et al., 1987). At low divalent cation concentrations poised to exist under physiological conditions, selectivity arises through strong divalent cation binding to high-affinity sites. As the divalent cation concentration is raised at the expense of monovalent ions, strong electrostatic repulsions between cations provide the driving force required for diffusion in the pore. Divalent permeation occurs as a compromise between strong coordination and high selectivity achieved by negative residues at the ligand site, whereas monovalent cation fluxes are not affected by the charge of the residues present at the same ligand site.

Kuo and Hess (1993a,b) pictured the calcium channel pore with high-affinity $Ca^{2+}$ binding sites close to the channel outer vestibule. Our mutational analysis identified two high-affinity $Ca^{2+}$ binding sites in the SS2 segment of the H5 region. Several negatively charged residues in this region have been implicated in the binding of cationic blockers such as charybdotoxin/agitoxin (MacKinnon and Miller, 1989; MacKinnon et al., 1990; Goldstein et al., 1994) and external tetraethylammonium (MacKinnon and Yellen, 1990; Kavanaugh et al., 1991) in voltage-dependent $K^+$ channels and in the binding of tetrodotoxin and saxitoxin in $Na^+$ channels (Terlau et al., 1991; Satin et al., 1992; Lipkind and Fozzard, 1994). Our results support the contention that negatively charged residues in the outer mouth represent a common architectural motif for $K^+$ (Kirsch et al., 1995) and $Ca^{2+}$ channels. This convergence of structure and function in voltage-dependent ion channels may extend to other regions of the pore. In calcium channels, low-affinity binding sites have been proposed to explain the "lock-in" effect experienced by $Ca^{2+}_i$ with increasing internal $Li^+$ (Kuo and Hess, 1993b). These low-affinity binding sites postulated to exist in the inner mouth of the calcium channel pore were not targeted in this study and remain to be identified. As in voltage-dependent $K^+$ channels, the inner mouth of the calcium channel pore might be formed by hydrophobic residues located in the cytoplasmic face of transmembrane segments S5 and S6 (Lopez et al., 1994; Shieh and Kirsch, 1994). Located deeper in the pore region, mutations in these low-affinity sites are expected to significantly affect the channel single-channel conductance.

We thank Dr. Michel de Waard for the rat brain $\alpha_{2b}$ subunit; W.-Q. Dong and R. Cockrell for oocyte injection and handling; M. Champagne, D. Davila, S. Chang, T. Rodriguez, C.-D. Zuo, and G. Cantrell for technical help; B. Steiner for the analysis software Eppro; Drs. G. E. Kirsch and A. E. Lacerda for discussions; and Dr. A. M. Brown for support and encouragement.

This work was supported in part by National Institutes of Health Grant HL37044 to A. M. Brown and by American Heart Association-Texas Affiliate Grant 94G-195 to Lucie Parent.

## REFERENCES


Almers, W., and E. W. McCleskey. 1984. Non-selective conductance in calcium channels of frog muscle: calcium selectivity in a single-file pore. *J. Physiol. (Lond.).* 353:585–608.

Almers, W., E. W. McCleskey, and P. T. Palade. 1984. A non-selective cation conductance in frog muscle membrane blocked by micromolar external calcium ions. *J. Physiol. (Lond.).* 353:565–583.

Armstrong, C. M., and J. Neyton. 1992. Ion permeation through calcium channels. A one site model. *Ann. N. Y. Acad. Sci.* 635:18–25.

Creighton, T. E. 1993. Proteins, Structures and Molecular Properties. W. H. Freeman and Company, New York.

DaSilva, J. J. R. F., and R. J. P. Williams. 1993. The Biological Chemistry of the Elements. Clarendon Press, Oxford.

Eismann, E., F. Müller, S. H. Heinemann, and U. B. Kaupp. 1994. A single negative charge within the pore region of a cGMP-gated channel controls rectification, $Ca^{2+}$ blockage, and ionic selectivity. *Proc. Natl. Acad. Sci. USA.* 91:1109–1113.

Fabiato, A., and F. Fabiato. 1979. Calculator programs for computing the composition of the solutions containing multiple metals and ligands used for experiments in skinned muscle cells. *J. Physiol. (Paris)* 75:463–505.

Goldstein, S. A. N., D. J. Pheasant, and C. Miller. 1994. The charybdotoxin receptor of a *Shaker* $K^+$ channel: peptide and channel residues mediating molecular recognition. *Neuron.* 12:1377–1388.

Hartmann, H. A., G. E. Kirsch, J. A. Drewe, M. Taglialatela, R. H. Joho, and A. M. Brown. 1991. Exchange of conduction pathways between two related $K^+$ channels. *Science.* 251:942–944.

Heinemann, S. H., H. Terlau, W. Stühmer, K. Imoto, and S. Numa. 1992. Calcium channel characteristics conferred on the sodium channel by single mutations. *Nature.* 356:441–443.

Hess, P., and R. W. Tsien. 1984. Mechanism of ion permeation through calcium channels. *Nature.* 309:453–456.

Hess, P., J. B. Lansman, and R. W. Tsien. 1986. Calcium channel selectivity for divalent and monovalent cations. Voltage and concentration dependence of single channel current in ventricular heart cells. *J. Gen. Physiol.* 88:293–319.

Kavanaugh, M. P., M. D. Varnum, P. B. Osborne, M. J. Christie, A. J. Busch, J. P. Adelman, and R. A. North. 1991. Interaction between tetraethylammonium and amino acid residues in the pore of cloned voltage-dependent potassium channels. *J. Biol. Chem.* 266:7583–7587.

Kim, M.-S., T. Mori, L.-X. Sun, K. Imoto, and Y. Mori. 1993. Structural determinants of ion selectivity in brain calcium channel. *FEBS Lett.* 318:145–148.

Kirsch, G. E., J. M. Pascual, and C.-C. Sheih. 1995. Functional role of a conserved aspartate in the external mouth of voltage-gated potassium channels. *Biophys. J.* 68:1804–1813.

Kuo, C.-C., and P. Hess. 1993a. Ion permeation through the L-type $Ca^{2+}$ channel in rat phaeochromocytoma cells: two sets of ion binding sites in the pore. *J. Physiol. (Lond.).* 466:629–655.

Kuo, C.-C., and P. Hess. 1993b. Characterization of the high-affinity $Ca^{2+}$ binding sites in the L-type $Ca^{2+}$ channel pore in rat phaeochromocytoma cells. *J. Physiol. (Lond.).* 466:657–682.

Lacerda, A. E., E. Perez-Reyes, X. Wei, A. Castellano, L. Birnbaumer, and A. M. Brown. 1994. T-type and N-type calcium channels of *Xenopus* oocytes: evidence for specific interactions with $\beta$ subunits. *Biophys. J.* 66:1833–1843.

Lansman, J. B., P. Hess, and R. W. Tsien. 1986. Blockade of current through single calcium channels by $Cd^{2+}$, $Mg^{2+}$, and $Ca^{2+}$. Voltage and concentration dependence of calcium entry into the pore. *J. Gen. Physiol.* 88:321–347.

Lansman, J. B. 1990. Blockade of current through single calcium channels by trivalent lanthanide cations. Effect of ionic radius on the rates of ions entry and exit. *J. Gen. Physiol.* 95:679–696.

Lipkind, G. M., and H. A. Fozzard. 1994. A structural model of the tetrodotoxin and saxitoxin binding site of the $Na^+$ channel. *Biophys. J.* 66:1–13.

Lopez, G. A, Y. N. Jan, and L. Y. Jan. 1994. Evidence that the S6 segment of the *Shaker* voltage-gated $K^+$ channel comprises part of the pore. *Nature.* 367:179–182.

Lux, H. D., E. Carbone, and H. Zucker. 1990. $Na^+$ currents through low-voltage-activated $Ca^{2+}$ channels of chick sensory neurones: block by external $Ca^{2+}$ and $Mg^{2+}$. *J. Physiol. (Lond.).* 430:159–188.

MacKinnon, R., and C. Miller. 1989. Mutant potassium channels with altered binding of charybdotoxin, a pore-blocking peptide inhibitor. *Science.* 245:1382–1385.

MacKinnon, R., and G. Yellen. 1990. Mutations affecting TEA blockade and ion permeation in voltage-activated $K^+$ channels. *Science.* 250: 276–279.

MacKinnon, R., L. Heginbotham, and T. Abramson. 1990. Mapping the receptor site for charybdotoxin, a pore-blocking potassium channel inhibitor. *Neuron.* 5:767–771.

McCleskey, E. W., and W. Almers. 1985. The Ca channel in skeletal muscle is a large pore. *Proc. Natl. Acad. Sci. USA.* 82:7149–7153.

Mikala, G., A. Bahinski, A. Yatani, S. Tang, and A. Schwartz. 1993. Differential contribution by conserved glutamate residues to an ion-selectivity site in the L-type $Ca^{2+}$ channel pore. *FEBS Lett.* 335: 265–269.

Mikami, A., K. Imoto, T. Tanabe, T. Niidome, Y. Mori, H. Takeshima, S. Narumiya, and S. Numa. 1989. Primary structure and functional expression of the cardiac dihydropyridine-sensitive calcium channel. *Nature.* 340:230–233.

Parent, L., D. Davila, M. Gopalakrishnan, and A. M. Brown. 1995a. Aspartate residue D737 in pore II of the cardiac calcium channel $\alpha_{1C}$ subunit contributes to high-affinity calcium and cadmium binding. *Biophys. J.* 68:264*a*. (Abstr.)

Parent, L., M. Gopalakrishnan, A. E. Lacerda, X. Wei, and E. Perez-Reyes. 1995b. Voltage-dependent inactivation in a cardiac-skeletal calcium channel chimera. *FEBS Lett.* 360:144–150.

Perez-Reyes, E., X. Wei, A. Castellano, and L. Birnbaumer. 1990. Molecular diversity of L-type calcium channels. Evidence for alternative splicing of the transcripts of three non-allelic genes. *J. Biol. Chem.* 265:20430–20436.

Perez-Reyes, E., A. Castellano, H. S. Kim, P. Bertrand, E. Baggstrom, A. E. Lacerda, X. Wei, and L. Birnbaumer. 1992. Cloning and expression of a cardiac/brain $\beta$ subunit of the L-type calcium channel. *J. Biol. Chem.* 267:1792–1797.

Pietrobon, D., B. Prod'hom, and P. Hess. 1989. Interactions of protons with single open L-type calcium channels. pH dependence of proton-induced current fluctuations with $Cs^+$, $K^+$, $Na^+$ as permeant ions. *J. Gen. Physiol.* 94:1–21.

Prod'hom, B., D. Pietrobon, and P. Hess. 1989. Interactions of protons with single open L-type calcium channels. Location of protonation site and dependence of proton-induced current fluctuations on concentration and species of permeant ion. *J. Gen. Physiol.* 94:23–42.

Root, M. J., and R. MacKinnon. 1993. Identification of an external divalent cation-binding site in the pore of a cGMP-activated channel. *Neuron.* 11:459–466.

Rosenberg, R. L., and X.-H. Chen. 1991. Characterization and localization of two ion-binding sites within the pore of cardiac L-type calcium channels. *J. Gen. Physiol.* 97:1207–1225.

Sambrook J., E. F. Fritsch, and T. Maniatis. 1989. Molecular cloning: a laboratory manual. Cold Spring Harbor Laboratory, Cold Spring Harbor, New York.

Sather, W. A., I., Nussinovitch, D. J. Gross, J. Yang, and R. W. Tsien. 1995. Altered multi-ion properties arising from mutations in the pore of an L-type $Ca^{2+}$ channel. *Biophys. J.* 68:130*a*. (Abstr.)

Satin, J., J. W. Kyle, M. Chen, P. Bell, L. L. Cribbs, H. A. Fozzard, and R. B. Rogart. 1992. A mutant of TTX-resistant cardiac sodium channels with TTX-sensitive properties. *Science.* 256:1202–1205.

Schultz, D., G. Mikala, A. Yatani, D. B. Engle, D. E. Iles, B. Segers, R. J. Sinke, D. O. Weghuis, U. Klöckner, M. Wakamori, J.-J. Wang, D. Melvin, G. Varadi, and A. Schwartz. 1993. Cloning, chromosomal localization, and functional expression of the $\alpha_1$ subunit of the L-type voltage-dependent calcium channel from normal human heart. *Proc. Natl. Acad. Sci. USA.* 90:6228–6232.

Shieh, C.-C., and G. E. Kirsch. 1994. Mutational analysis of ion conduction and drug binding sites in the inner mouth of voltage-gated $K^+$ channels. *Biophys. J.* 67:2316–2325.

Tang, S., G. Mikala, A. Bahinski, A. Yatani, G. Varadi, and A. Schwartz. 1993. Molecular localization of ion selectivity sites within the pore of a

human L-type cardiac calcium channel. *J. Biol. Chem.* 268: 13026–13029.

Terlau, H. S., S. H. Heinemann, W. Stühmer, M. Pusch, F. Conti, K. Imoto, and S. Numa. 1991. Mapping the site of block by tetrodotoxin and saxitoxin of sodium channel II. *FEBS Lett.* 293:93–96.

Tsien, R. W., P. Hess, E. W. McCleskey, and R. L. Rosenberg. 1987. Calcium channels: mechanisms of selectivity, permeation, and block. *Annu. Rev. Biophys. Biophys. Chem.* 16:265–290.

Wei, X., A. Neely, A. E. Lacerda, R. Olcese, E. Stefani, E. Perez-Reyes, and L. Birnbaumer. 1994a. Modification of $Ca^{2+}$ channel activity by deletions at the carboxyl terminus of the cardiac $\alpha_1$ subunit. *J. Biol. Chem.* 269:1635–1640.

Wei, X., A. Neely, R. Olcese, E. Stefani, and L. Birnbaumer. 1994b. Gating and ionic currents from N-terminal deletion mutants of the cardiac $Ca^{2+}$ channel $\alpha_1$ subunit. *Biophys. J.* 66:128*a*. (Abstr.)

Yang, X.-C., and F. Sachs. 1989. Block of stretch-activated ion channels in *Xenopus* oocytes by gadolinium and calcium ions. *Science.* 243: 1068–1071.

Yang, J., P. T. Ellinor, W. A. Sather, J. F. Zhang, and R. W. Tsien. 1993. Molecular determinants of $Ca^{2+}$ selectivity and ion permeation in L-type $Ca^{2+}$ channels. *Nature.* 366:158–161.

Yatani, A., A. Bahinsky, G. Mikala, S. Yamamoto, and A. Schwartz. 1994. Single amino acid substitutions within the ion permeation pathway alter single-channel conductance of the human L-type cardiac $Ca^{2+}$ channel. *Circ. Res.* 75:315–323.

Yool, A. J., and T. L. Schwarz. 1991. Alteration of ionic selectivity of a $K^+$ channel by mutation of the H5 region. *Nature.* 349:700–704.

Yue, D. T., and E. Marban. 1990. Permeation in the dihydropyridine-sensitive calcium channel. Multi-ion occupancy but no anomalous mole-fraction effect between $Ba^{2+}$ and $Ca^{2+}$. *J. Gen. Physiol.* 95:911–939.